



## RESEARCH ARTICLE

# Design and synthesis of peptides as stabilizers of histone deacetylase 4

Annika Lill<sup>1</sup> | Markus Schweipert<sup>2</sup> | Thomas Nehls<sup>3</sup> | Eva Wurster<sup>2</sup> |  
Frederik Lermyte<sup>3</sup> | Franz-Josef Meyer-Almes<sup>2</sup>  | Katja Schmitz<sup>1</sup> 

<sup>1</sup>Biological Chemistry, Clemens-Schöpf-Institute of Organic Chemistry and Biochemistry, Technical University of Darmstadt, Darmstadt, Germany

<sup>2</sup>Physical Biochemistry, Chemical Engineering and Biotechnology, University of Applied Sciences Darmstadt, Darmstadt, Germany

<sup>3</sup>Conformation-Sensitive Mass Spectrometry Laboratory, Clemens-Schöpf-Institute of Organic Chemistry and Biochemistry, Technical University of Darmstadt, Darmstadt, Germany

**Correspondence**

Katja Schmitz, Biological Chemistry, Clemens-Schöpf-Institute of Organic Chemistry and Biochemistry, Technical University of Darmstadt, Peter-Grünberg-Straße 8, 64287 Darmstadt, Germany.  
Email: [katja.schmitz@tu-darmstadt.de](mailto:katja.schmitz@tu-darmstadt.de)

Franz-Josef Meyer-Almes, Physical Biochemistry, Chemical Engineering and Biotechnology, University of Applied Sciences Darmstadt, Stefanstraße 7, 64295 Darmstadt, Germany.  
Email: [franz-josef.meyer-almes@h-da.de](mailto:franz-josef.meyer-almes@h-da.de)

**Funding information**

Hessisches Ministerium für Wissenschaft und Kunst; Deutsche Forschungsgemeinschaft, Grant/Award Numbers: INST163/445-1FUGG, 461372424

Histone deacetylase 4 (HDAC4) contributes to gene repression by complex formation with HDAC3 and the corepressor silencing mediator for retinoid or thyroid hormone receptors (SMRT). We hypothesized that peptides derived from the class IIa specific binding site of SMRT would stabilize a specific conformation of its target protein and modulate its activity. Based on the SMRT-motif 1 (SM1) involved in the interaction of SMRT with HDAC4, we systematically developed cyclic peptides that exhibit  $K_d$  values that are 9 to 56 times lower than that of the linear SMRT peptide. The peptide macrocycles stabilize the wildtype of the catalytic domain of HDAC4 (cHDAC4) considerably better than its thermally more stable ‘gain-of-function’ (GOF) variant, cHDAC4-H976Y. Molecular docking and mutagenesis studies indicated that the cyclic peptides bind in a similar but not identical manner as the linear SMRT peptide to a discontinuous binding site. Ion mobility mass spectrometry showed no major changes in the protein fold upon peptide binding. Consistent with these results, preliminary hydrogen-deuterium exchange mass spectrometry measurements indicated only minor conformational changes. Taken together, the cyclic SMRT peptides most likely stabilize the apo form of cHDAC4.

**KEYWORDS**

binding peptide, conformational stabilization, cyclization, histone deacetylase

**Abbreviations:** Bip, 3-(4-biphenyl)-L-alanine; Bpa, 4-benzoyl-L-phenylalanine; cHDAC4, catalytic domain of histone deacetylase 4; HATU, 1-[bis(dimethylamino)methylene]-1H-1,2,3-triazolo[4,5-b]pyridinium 3-oxide hexafluorophosphate; HDAC4, histone deacetylase 4; HDAC4 GOF, gain-of-function variant of histone deacetylase 4; HDX-MS, hydrogen deuterium exchange mass spectrometry; HOAt, 1-hydroxy-7-azabenzotriazole; IM-MS, ion-mobility mass spectrometry; Nal, 3-(1-naphthyl)-L-alanine; NCoR, nuclear receptor corepressor; NMM, N-methylmorpholine; Phg, L-phenylglycine; RD, repressor domain; SM1, SMRT motif 1; SMRT, silencing mediator for retinoid or thyroid hormone receptors; SP1, SMRT peptide 1; TAMRA, 5(6)-carboxytetramethylrhodamine.

This is an open access article under the terms of the [Creative Commons Attribution](https://creativecommons.org/licenses/by/4.0/) License, which permits use, distribution and reproduction in any medium, provided the original work is properly cited.

© 2024 The Authors. *Journal of Peptide Science* published by European Peptide Society and John Wiley & Sons Ltd.

## 1 | INTRODUCTION

Lysine acetylation is a posttranslational protein modification that affects protein activity and function.<sup>1</sup> Histone deacetylases (HDACs) are a class of enzymes capable of removing a posttranslationally added acetyl group from lysine residues in histones and other target proteins.<sup>2–5</sup> HDACs are divided into two families based on their cofactors and further divided into subclasses according to their similarity to yeast protein.<sup>2,4–8</sup>

Human HDAC4 belongs to class IIa HDACs. It is primarily expressed in brain, heart, and skeletal muscle tissue and plays a major role in tissue growth and physiological development.<sup>8</sup>

The size ranges from 972 to 1084 amino acids.<sup>8,9</sup> HDAC4 contains two zinc ions, one catalytic zinc ion in the active site and the other in the structural zinc-binding domain, which is known to be highly flexible.<sup>10</sup> Like all class IIa HDACs, HDAC4 shows low enzymatic activity due to a histidine residue in the active site, which in class I HDACs is a tyrosine.<sup>7,11</sup> The deacetylase activity of HDAC4 can be restored by an H976Y mutation. This substitution produces the so-called *gain-of-function* variant of HDAC4 (HDAC4 GOF), which is widely used in research because of its enzymatic activity and increased stability compared with the wildtype.<sup>11</sup>

Due to the low enzymatic activity, the main role of class IIa family members is to act as a platform for the interaction of transcription factors and corepressors that coordinate the activity of class I HDACs.<sup>12</sup> For this purpose, class IIa HDACs feature an N-terminal extension of 450–600 amino acids, which comprises binding sites for different transcription factors.<sup>13</sup>

The most important role of class IIa HDACs lies in the recruitment of a multiprotein complex containing HDAC3 and the corepressor silencing mediator for retinoid or thyroid hormone receptors (SMRT) also known as the nuclear receptor corepressor (NCoR).<sup>3,4,6,13</sup> The current model assumes that HDAC4 binds with its extended N-terminal domain to the DNA-binding transcription factor MEF2 and then recruits the SMRT/NCoR-HDAC3 complex.<sup>3,13,14</sup> Mutagenesis studies have revealed that the rim of the catalytic entry site of HDAC4 is the major binding surface for SMRT.<sup>15</sup> SMRT has three different so-called repressor domains (RD), each binding to a different target protein. RD1 binds mSin3A, which in turn recruits class I HDAC1 and 2, RD2 binds HDAC3, whereas RD3 binds to different class IIa HDACs, such as HDAC4, 5, and 7.<sup>16</sup>

Sequence analysis of RD3 from SMRT and NCoR RD3 revealed several motifs, starting with a glycine-serine-isoleucine triad (GSI-motif).<sup>17</sup> The so-called SMRT-motif-1 (SM1; <sup>1361</sup>GSITQGIPR<sup>1369</sup>) and SMRT-motif-2 (SM2; <sup>1457</sup>GSITQGTPL<sup>1465</sup>) were found to be essential for HDAC4 binding, with SM1 being the more important one. Two peptides containing the SM1 (SP1, SMRT peptide 1) and the SM2 sequence (SP2, SMRT peptide 2), respectively, were cocrystallized with the catalytic domain of HDAC4 GOF (PDB: 5ZOO, 5ZOP). The peptides were bound in the cleft leading to the active site adopting a hairpin-like conformation.<sup>18</sup>

HDAC4 is recognized as a target for neurodegenerative diseases, in particular Huntington's disease,<sup>19,20</sup> and in different types of cancer.<sup>9,21</sup> Therefore, class IIa HDACs are a well-studied protein family for which several inhibitors have been developed.

Most HDAC inhibitors are unselective pan-inhibitors for all zinc-dependent HDACs and contain a hydroxamic acid as a zinc-binding group. Five of them have already been approved as drugs by the FDA, namely, Vorinostat (Zolinza<sup>®</sup>), Panobinostat (Farydak<sup>®</sup>), Belinostat (Beleodaq<sup>®</sup>), Romidepsin (Istodax<sup>®</sup>), and Tucidinostat (Epidaza<sup>®</sup>).<sup>22–25</sup> Due to the poor selectivity and potential mutagenic effects of hydroxamic acids, the search for alternative HDAC inhibitors is

paramount.<sup>26</sup> The first small-molecule HDAC4 inhibitors with non-hydroxamate warheads and improved isozyme selectivity have been described.<sup>27–29</sup> However, inhibitors that block the entrance to the active site and prevent the formation of the SMRT/NCoR-HDAC3/HDAC4 complex may be more specific and biologically active as class IIa inhibitors than classic active site binders.<sup>20</sup>

Therefore, we set out to improve the binding properties of SM1-derived peptides with regard to inhibition and stabilization. We systematically developed peptide derivatives and tested their effect on the WT and GOF variant of cHDAC4. We hypothesized that SM1-derived peptides, like SMRT itself, should bind and stabilize the active conformation of cHDAC4 and block the entry to the active site.

## 2 | MATERIAL AND METHODS

### 2.1 | Mutagenesis, recombinant production, and purification of cHDAC4 wildtype and variants

The catalytic domain of human HDAC4 (cHDAC4, T648-T1057) and the gain-of-function variant were produced in *Escherichia coli* BL21 (DE3) utilizing a pET14b vector containing the HDAC4 gene fused with a His<sub>6</sub>-SUMO tag. Note, due to the combination of the SUMO tag and the NdeI restriction enzyme cleavage site, the used cHDAC4 construct exhibited two additional amino acids (H and M) before T648 at the N-terminus.

All cHDAC4 variants were generated with the splicing by overlap extension polymerase chain reaction (SOE-PCR) method utilizing the mutagenesis primers listed in Table 1.<sup>30</sup> Nucleic acid sequences of variants were verified by sequencing done by the faculty of biology of Ludwig Maximilian University of Munich, Germany.

For all proteins, expression was carried out in autoinduction media over night at 30°C. Cells were lysed by sonification, and the protein was enriched from the lysate supernatant by IMAC (5-mL cComplete His-Tag Purification Resin, Roche, Basel, Switzerland). The His<sub>6</sub>-SUMO-tag was cleaved by SUMO protease overnight and removed by HIC purification. (5-mL Toyopearl Butyl-650M, Tosoh Bioscience, Tokyo, Japan). As a final step, size exclusion chromatography (SEC, HiLoad Superdex 16/600 75 pg, Cytiva, Marlborough, United States) was performed. A detailed description can be found in the [Supporting Information](#).

### 2.2 | IC<sub>50</sub> determination

A serial dilution of the respective ligand was prepared in assay buffer (25 mM Tris-HCl, 75 mM KCl, 0.00001% Pluronic F-68, pH 8) and incubated with 1 nM cHDAC4 WT or 10 nM cHDAC4 GOF in a black 96-well microtiter plate (Greiner, Kremsmünster, Austria). Subsequently the enzymatic reaction was initiated by the addition of 20 μM Boc-Lys{TFA}-7-amino-4-methylcoumarin (Bachem, Bubendorf, Switzerland) and 50 μM Boc-Lys[Ac]-7-amino-4-methylcoumarin (Bachem, Bubendorf, Switzerland) as substrate for cHDAC4 WT and

**TABLE 1** Primer sequences for cHDAC4 variants.

Primer cHDAC4 variant	5'-sequence-3'
D757A for	GTTGGCGTGGCTAGTGATACCATTGGAATGAAGT
D757A rev	GTATCACTAGCCACGCCAACACCGCCACACGGCAG
S758A for	GTTGGTGTCTGATGCTGACACCATCTGG
S758A rev	CCAGATGGTGTGACATCGACACCAAC
D759A for	GGTGTCTGATTCTGCTACCATCTGGAAC
D759A rev	GTTCCAGATGGTAGCAGAATCGACACC
P809A for	GAAAGTACCGCTATGGGCTTTTGTATTTTAATAG
P809A rev	AAGCCCATAGCGGTACTTCTTCTGCATGATGACC
F812A for	ACGCCGATGGGTGCTTGCTATTTCAAT
F812A rev	ATTGAAATAGCAAGCACCCATCGGCCGT
F872A for	AATTTCTTTGCTGGTAGTGGCGCACCGGATGAAGT
F872A rev	CCACTACCAGCAAAGAAATTACCATCATCATAACG
F871A for	GACGGCAACTTTGCTCCGGGCAGTGGT
F871A rev	ACCACTGCCCGGAGCAAAGTTGCCGTC
L943A for	CATCCGACCCCGGCTGGCGTTATAAC
L943A rev	GTTATAACCGCCAGCCGGGGTCCGGATG
H976Y for	CTGGAAGGTGGTTATGATCTGACCCGA
H976Y rev	TGCGGTCAGATCATAACCACCTTCCAG

cHDAC4 GOF, respectively. After another incubation step, the enzymatic reaction was terminated by the addition of 1.7  $\mu\text{M}$  SATFMK and the deacetylated substrate was cleaved to yield its fluorescent product by the addition of 0.4  $\mu\text{M}$  trypsin (AppliChem, Darmstadt Germany). The amount of fluorescent product was measured in a microplate reader (PheraStar Optima, BMG Labtech, Ortenberg, Germany) at 450 nm ( $\lambda_{\text{Ex}} = 350$  nm) and correlated to enzyme activity. GraphPad Prism was used to generate dose response curves, which were fitted to a four-parameter logistic function to obtain  $\text{IC}_{50}$  values<sup>31</sup>:

$$EA = E_0 + \frac{(E_{\text{max}} - E_0)}{1 + 10^{\log(\text{IC}_{50}) - x \cdot h}}$$

in which EA is the enzyme activity for a given inhibitor concentration  $x$ ,  $E_{\text{max}}$  and  $E_0$  are the enzyme activities in the absence of inhibitor and at complete inhibition, respectively.  $h$  is the slope of the curve and  $\text{IC}_{50}$  is the inhibitor concentration at which half of the enzyme activity is inhibited. All incubations steps were performed on a shaker for 1 h at 30°C and 450 rpm.  $\text{IC}_{50}$  values were converted to  $K_i$  values using the Cheng–Prusoff equation for competitive inhibitors<sup>32</sup>:

$$K_i = \frac{\text{IC}_{50}}{1 + \left(\frac{S}{K_m}\right)}$$

where  $K_i$  is the inhibitor binding affinity,  $\text{IC}_{50}$  is the inhibition determined using the  $\text{IC}_{50}$  assay,  $S$  is the substrate concentration, and  $K_m$  is the Michaelis constant of the enzyme–substrate pair. Michaelis–Menten plots are provided in the Supporting Information (Figure S5).

### 2.3 | Differential scanning fluorimetry

For determination of the thermal stabilization, a mixture containing 10  $\mu\text{M}$  of protein, 100  $\mu\text{M}$  of the respective ligand, and a 10-fold concentration of SYPRO Orange fluorescence dye was incubated in a RT-qPCR device (QuantStudio 5, Thermo Fisher, Waltham, United States) at 30°C for 1 h, followed by a temperature decrease to 25°C for 2 min. Subsequently, the temperature was increased from 25°C to 95°C with a ramp rate of 0.015°C/s, and the change in fluorescence intensity of SYPRO Orange was recorded with the RT-qPCR device's TAMRA channel. For melting point determination, the first derivative of the melting curve was calculated by Thermo Fisher's Protein Thermal Shift Software and plotted against the respective temperature where the melting point,  $T_M$ , equals the maximum.

### 2.4 | Statistical analysis

$\text{IC}_{50}$  values were calculated from 10 different concentrations, which were created by serial dilution starting with 35  $\mu\text{M}$  for the highest concentration. Data were fit to the four-parameter logistic equation given in subsection  $\text{IC}_{50}$  determination using nonlinear regression and GraphPad Prism software. The quality was assessed by calculating the Goodness of Fit and R2. The standard error SE of  $\text{IC}_{50}$  values was calculated on the basis of the entire set of 10 data points according to the following equation:

$$E(P_i) = \sqrt{\frac{SS}{df} \text{Cov}(i,i)}$$

where  $P_i$  is the  $i$ -th adjustable parameter (in our case  $IC_{50}$ ),  $SS$  represents the sum of squared residuals,  $df$  stands for degrees of freedom (number of data points minus number of parameters fit by regression), and  $Cov(i,i)$  is the  $i$ -th diagonal element of the covariance matrix. Mean and SE were transformed into  $K_i$  values as described above.

Melting temperatures of HDAC4 in the absence and in the presence of peptide ligands were determined with high precision of about  $\pm 0.2^\circ\text{C}$  and calculated using Thermo Fisher's Protein Thermal Shift Software. Mean and SE were calculated from four replicates.

## 2.5 | Synthesis of linear peptides

Linear peptides were synthesized manually on Fmoc-Rink-amide-AM resin (0.63 mmol/g, Carbolution, St. Ingbert, Germany) or for linear cyclic precursor peptides on TentaGel R RAM resin (0.18 mmol/g, Rapp Polymere GmbH, Tübingen, Germany) using the standard Fmoc/tBu strategy. See [Supporting Information](#) (section S7.1) for details.

## 2.6 | Synthesis of cyclic peptides

Linear precursor peptides were synthesized as described above. For head-to-tail cyclized peptides, the first amino acid introduced was Fmoc-Glu-OAll or Fmoc-Asp-OAll through side chain anchoring on the solid support and for side-chain-to-tail cyclized peptides Fmoc-Glu(OAll)-OH or Fmoc-Asp(OAll)-OH was introduced first. After the synthesis of the remaining peptide sequence, the allyl group was removed by treating the resin three times for 30 min each with a freshly prepared solution of 1 eq. tetrakis (triphenylphosphin)-palladium(0) and 10 eq. phenylsilane in DCM/acetic acid/*N*-methylmorpholine (23:2:1 [v:v:v]). To remove the catalyst the resin was washed alternating with a solution of 0.5% sodium diethylcarbamoyldithioate in DMF and 0.5% *N,N*-diisopropylethylamine (DIEA) in DMF until the wash solution remained colourless and subsequently three times with DMF. Afterwards, the *N*-terminal Fmoc-protecting group was removed as described previously. For cyclization, 10 equivalents of 1-[bis (dimethylamino)methylene]-1*H*-1,2,3-triazolo[4,5-*b*]pyridinium 3-oxide hexafluorophosphate (HATU), 10 equivalents of 1-hydroxy-7-azabenzotriazole (HOAt), and 20 equivalents of *N*-methylmorpholine (NMM) in DMF were added to the resin twice for 1 h each. The resin was washed, and the peptide was deprotected and cleaved from solid support as described in the [Supporting Information](#), section S7.

## 2.7 | Affinity determination by fluorescence anisotropy

Fluorescence anisotropy measurements were performed on an Infinite M1000 microplate reader (Tecan, Zürich, Switzerland) using low-volume black, clear/flat-bottom 384-well microtiter plates (Corning, New York, United States). cHDAC4 WT and GOF were prepared in

12 consecutive 1:2 dilutions of protein in assay buffer (25 mM Tris-HCl, 75 mM KCl, 0.000001% Pluronic, pH 8.0) to give final volumes of 31.5  $\mu\text{L}$ ; 3.5  $\mu\text{L}$  of the fluorescent-labelled peptide or TAMRA (250 nM) was added. As negative control, 31.5  $\mu\text{L}$  of buffer with 3.5  $\mu\text{L}$  of fluorescent-labelled peptide or TAMRA was prepared. Additionally, a blank with plain buffer was prepared. The mixtures were gently mixed and incubated for 1 h in the dark; 10  $\mu\text{L}$  of each solution were transferred into three adjacent cavities of the 384-well microtiter plate resulting in technical triplicates. The fluorescence anisotropy was measured at  $\lambda_{\text{ex}} = 530 \text{ nm}$  and  $\lambda_{\text{em}} = 579 \text{ nm}$ . Binding data were evaluated by nonlinear regression in GraphPad Prism (Version 9.5, GraphPad Software, LLC) by fitting to the "Agonist vs. Response variable Hillslope":

$$Y = \min * \frac{X^{\text{Hillslope}} * (\max - \min)}{(X^{\text{Hillslope}} + K_D^{\text{Hillslope}})}$$

Min and max are the minimum and maximum fluorescence anisotropy,  $Y$  is the measured fluorescence anisotropy, and  $X$  is the concentration of cHDAC4 in  $\mu\text{M}$ . The standard error of the  $K_D$  was calculated in the same fashion as described for the  $IC_{50}$  values in the statistical analysis section.

## 3 | RESULTS AND DISCUSSION

### 3.1 | Design of SM1-derived peptides

We started out from the previously reported SM1 sequence (GSITQGIPR). We wanted to compare its affinity to that reported for the SMRT Peptide 1 (SP1, HIRGSITQGIPRSYV), which was used by Park et al. in 2018 for crystallization and has a reported  $K_D$  of 2.23  $\mu\text{M}$  towards cHDAC4 GOF.<sup>33</sup>  $K_D$  values determined by fluorescence anisotropy measurements with an *N*-terminally TAMRA-labelled SM1-peptide were somewhat higher than those of the SP1-peptide but still in the low micromolar range for both cHDAC4 WT and GOF. We also tested the labelled and unmodified SM1 and SP1 peptides on their ability to inhibit both proteins and found that the unlabelled SM1 peptide was a weaker inhibitor than SP1 but that the fluorophore-labelled SM1 peptide had a  $K_i$  value similar to the SP1 peptide (Table 2). Although the fluorophore alone does not bind cHDAC4 (Figure S1), comparison to the unmodified SM1 peptide demonstrates that it increases inhibition by the labelled peptide.

The original SP1 sequence features the sequence HIR at the *N*-terminus, and the crystal structure of the HDAC4:SP1 complex (PDB-ID: 5ZOO) reveals that the arginine residue points to the surrounding medium and does not form any contacts with the protein. We hypothesized that hydrophobic residues could form additional contacts that would account for the observed improvement of affinity. We therefore sought to improve SM1 affinity by adding hydrophobic residues. As the crystal structure of SP1 with cHDAC4 GOF<sup>18</sup> shows that both termini protrude from the binding site in a similar

direction, residues were added to either side of the SM1 peptide sequence to test if amino acids at these positions could increase the affinity, similar to TAMRA.

Tryptophan and phenylalanine were chosen because of their large hydrophobic side chain and alanine for its small side chain. The

**TABLE 2** Affinity and inhibition values of SP1, SM1, and its labelled derivative. Inhibition values are from single measurements. Dissociation constants and standard deviation are from technical triplicate measurements (n.a. not applicable; SM1 = GSITQGIPR; SP1: HIR-SM1-SYV).

	$K_D/\mu\text{M}$		$K_i/\mu\text{M}$	
	WT	GOF	WT	GOF
SM1	n.a	n.a	14.3 ± 1.1	8.2 ± 1.8
SP1	n.a	2.23 <sup>a</sup>	5.5 ± 1.4	1.2 ± 0.3
TAMRA-SM1	5.4 ± 0.3	7.7 ± 0.3	5.3 ± 0.9	1.6 ± 0.4

<sup>a</sup> $K_D$  for SP1 towards cHDAC4 GOF was taken from Park et al.<sup>18</sup>

**TABLE 3** Inhibition and stabilization data of SM1 peptides with one additional N- or C-terminal amino acid towards cHDAC4 WT ( $T_M \approx 54^\circ\text{C}$ ) and GOF ( $T_M \approx 62^\circ\text{C}$ ). Mean and standard deviation of the thermal stabilization data come from technical quadruplicates.

	$K_i/\mu\text{M}$		$\Delta T_M/^\circ\text{C}$	
	WT	GOF	WT	GOF
SM1	14.3 ± 1.1	8.2 ± 1.8	2.89 ± 0.08	0.45 ± 0.08
W-SM1	12.9 ± 1.1	3.1 ± 0.4	3.39 ± 0.13	1.09 ± 0.24
F-SM1	14.7 ± 1.8	4.1 ± 0.6	3.32 ± 0.08	0.91 ± 0.07
A-SM1	21.3 ± 7.5	6.9 ± 1.3	3.36 ± 0.06	0.73 ± 0.08
SM1-W	16.3 ± 1.5	5.4 ± 0.7	3.35 ± 0.07	1.02 ± 0.16
SM1-F	16.4 ± 3.5	4.4 ± 0.6	3.57 ± 0.15	1.09 ± 0.08
SM1-A	31.9 ± 4.5	9.6 ± 1.7	2.45 ± 0.08	0.38 ± 0.01

**TABLE 4** Inhibition and stabilization data of cyclic SM1 and W-SM1 variants. The best stabilizer and inhibitor peptides are highlighted in bold. The C-terminally added amino acid specifies the used cyclization method and the nature of the amino acid side chain after cleavage. E/D: side-chain-to-tail cyclization; Q/N: head-to-tail-cyclization, c: cyclic. Mean and standard deviation of the thermal stabilization data come from technical quadruplicates.

	$K_i/\mu\text{M}$		$\Delta T_M/^\circ\text{C}$	
	WT	GOF	WT	GOF
SM1	14.3 ± 1.1	8.2 ± 1.8	2.89 ± 0.08	0.45 ± 0.08
cSM1-E	16.0 ± 3.0	4.7 ± 1.1	2.92 ± 0.15	0.74 ± 0.08
cSM1-D	10.1 ± 1.3	3.0 ± 0.8	<b>5.89 ± 0.07</b>	<b>1.09 ± 0.16</b>
cSM1-Q	<b>7.9 ± 0.9</b>	<b>2.1 ± 0.4</b>	4.45 ± 0.18	0.98 ± 0.07
cSM1-N	15.3 ± 2.4	4.6 ± 0.6	2.66 ± 0.07	0.42 ± 0.07
cW-SM1-E	<b>0.56 ± 0.11</b>	<b>0.29 ± 0.14</b>	<b>7.05 ± 0.07</b>	<b>3.44 ± 0.21</b>
cW-SM1-D	3.6 ± 0.6	1.3 ± 0.4	5.35 ± 0.05	2.45 ± 0.07
cW-SM1-Q	4.2 ± 0.4	1.6 ± 0.3	4.41 ± 0.06	1.16 ± 0.24
cW-SM1-N	5.8 ± 0.8	2.4 ± 0.5	3.70 ± 0.08	1.02 ± 0.07

peptides were tested both for inhibition and for stabilization of cHDAC4 WT and GOF.

No peptide exhibited lower  $K_i$  values than the TAMRA-SM1 peptide (Table 3). Towards the WT, N-terminally added amino acids led to no improvement of inhibition and only slightly improved stabilization. For the GOF, all N-terminally modified peptides had lower  $K_i$  values than the SM1 peptide, and stabilization was improved. The largest improvements were found for W-SM1 with a  $K_i$  value for the GOF close to that of TAMRA-SM1. The addition of more than one amino acid to the N-terminus did not lead to further improved stabilization or inhibition of cHDAC4 (Table S1). In general, modifications at the N-terminus had a slightly larger effect than C-terminal modifications. Only low stabilization of up to  $1^\circ\text{C}$  was obtained for the GOF, which is in accordance with the higher stability of this variant.

To constrain the SM1-derived peptides to the observed hairpin structure, and in the process enhance their affinity by decreasing their conformational flexibility, cyclic variants of SM1 and W-SM1 were synthesized.<sup>34,35</sup> Two different cyclization methods were employed, head-to-tail cyclization and side chain-to-tail cyclization. For head-to-tail cyclization, side chain anchoring of a glutamic or aspartic acid was employed. After cyclization, upon cleavage, the side chain was transformed to an amide and therefore represents the side chain of glutamine (Q) or asparagine (N). For side-chain-to-tail cyclization, the cycle was formed with the side chain of glutamic (E) or aspartic acid (D) (peptide structures can be found in the Supporting Information, section S7.4). This yielded ring sizes of 30 to 32 for cSM1-X and 33 to 35 for cW-SM1-X.

As summarized in Table 4, cyclic variants of W-SM1 were better stabilizers and inhibitors for WT and GOF than cyclic SM1 variants. cW-SM1-E even exhibited  $K_i$  values in the nanomolar range and stabilization of the WT up to  $7^\circ\text{C}$ . Nevertheless, cSM1-E and cW-SM1-D were similar in terms of stabilization of the WT.

To examine the role of the side-chain of the N-terminally added amino acid, cyclic peptides of the general formula cX-SM1-E with smaller amino acid side chains (L-alanine, L-valine, L-phenylglycine

[Phg], L-phenylalanine) and similar or larger side chains (3-(1-naphthyl)-L-alanine (Nal), 3-(4-biphenyl)-L-alanine (Bip), 4-benzoyl-L-phenylalanine (Bpa)) at the former tryptophan position were synthesized and tested.

Compared with SM1, all peptides of the cX-SM1-E series showed improved inhibition and stabilization towards WT and GOF with  $K_i$  values mostly in the low micromolar to high nanomolar range and stabilization of the WT between 5.7°C and 7.9°C and between 3.4°C and 5.9°C for GOF (Table 5). Interestingly, cF-SM1-E showed a three to eight times higher  $K_i$  to WT than the other peptides but did not differ from the other peptides in GOF inhibition. In terms of stabilization of WT, both cF-SM1-E and cPhg-SM1-E showed less improvement than the other peptides leading to the assumption that there might be different binding modes for peptides with large side chains and small ones. Phenylalanine and phenylglycine with a medium-sized side chain may not be able to adjust to either of these modes and consequently are not able to stabilize the protein to the same degree as the others.

### 3.2 | Characterization of peptide-cHDAC4 complexes

To confirm that the peptides bind at the entrance to the active site, which is also the binding site of precursor protein SMRT and precursor peptide SP1,<sup>15,18</sup> a fluorescent probe that binds to the active site was utilized as a tracer in competition experiments based on fluorescence anisotropy.<sup>36</sup> The selected peptides competed for the active site of WT and GOF considerably better than SM1, albeit to a lesser extent than the known active-site binding inhibitor SATFMK,<sup>37</sup> which is in accordance with the  $K_i$  values of these inhibitors (Figure S6).

To identify potential interactions between the peptides and cHDAC4, rigid docking was utilized. The crystal structure of the SP1 in complex with cHDAC4 GOF (PDB: 5ZOO) served as a template. The procedure was validated by successful redocking of the SP1 peptide into the cHDAC4 receptor (RMSD = 0.95 Å; Figure S7). Rigid docking has considerable limitations, because induced conformational

**TABLE 5** Inhibition and stabilization data of cyclic cX-SM1-E peptides. The best stabilizer and inhibitor peptides are highlighted in bold. Mean and standard deviation of the thermal stabilization data come from technical quadruplicates.

	$K_i/\mu\text{M}$		$\Delta T_M/^\circ\text{C}$	
	WT	GOF	WT	GOF
SM1	14.3 ± 1.1	8.2 ± 1.8	2.89 ± 0.08	0.45 ± 0.08
cA-SM1-E	0.93 ± 0.11	0.15 ± 0.09	7.40 ± 0.07	3.43 ± 0.01
cV-SM1-E	1.3 ± 0.2	0.18 ± 0.11	<b>7.91 ± 0.08</b>	<b>5.91 ± 0.08</b>
cPhg-SM1-E	1.1 ± 0.6	0.89 ± 0.33	5.74 ± 0.26	3.99 ± 0.37
cF-SM1-E	4.9 ± 1.6	0.70 ± 0.23	5.67 ± 0.24	4.20 ± 0.29
cW-SM1-E	<b>0.56 ± 0.11</b>	<b>0.29 ± 0.14</b>	7.05 ± 0.07	3.44 ± 0.21
cNal-SM1-E	<b>0.56 ± 0.09</b>	<b>0.18 ± 0.12</b>	<b>7.28 ± 0.02</b>	3.82 ± 0.13
cBip-SM1-E	1.6 ± 0.6	0.22 ± 0.07	6.86 ± 0.02	3.50 ± 0.08
cBpa-SM1-E	1.2 ± 0.3	0.26 ± 0.08	7.04 ± 0.07	<b>5.14 ± 0.01</b>

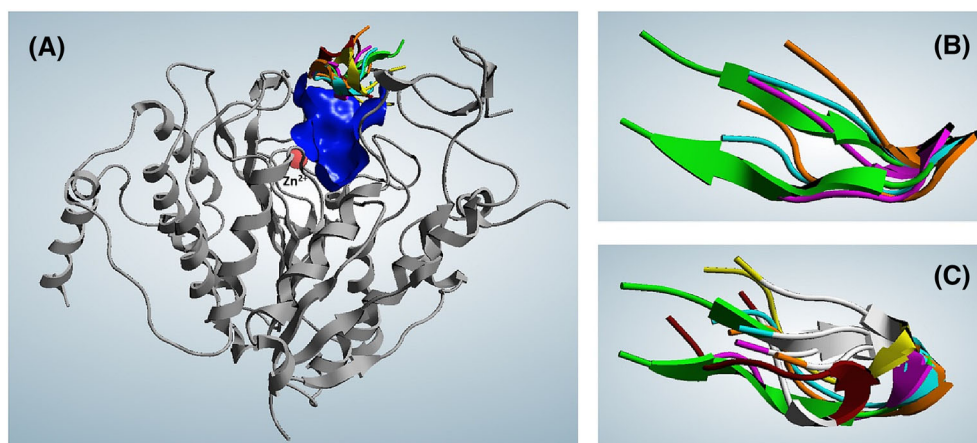
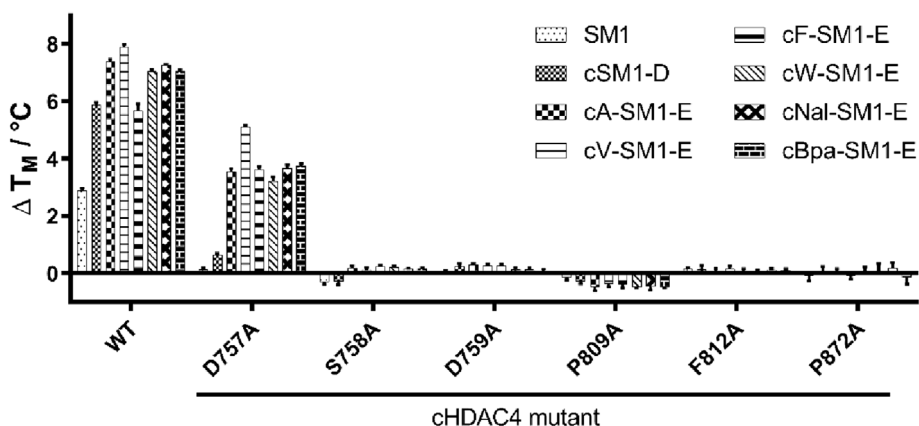


**FIGURE 1** Suggested binding poses of SP1 (green), cA-SM1-E (magenta), cV-SM1-E (orange), cF-SM1-E (cyan), cW-SM1-E (yellow), and cNal-SM1-E (brown) to HDAC4 (PDB-ID 5ZOO). (A) Overall view, (B) enlarged overlay of superposed peptides SP1, cA-SM1-E, cF-SM1-E and cV-SM1-E show similar binding poses with particularly close overlap in the loop with GSI-motif. (C) Enlarged overlay of superposed SP1, cW-SM1-E, and cNal-SM1-E, which show different binding poses. The GSI-motifs in these peptides (in white) differ clearly from that of SP1. The active centre is indicated by a dark blue surface.

**FIGURE 2** Stabilization data of cHDAC4 variants by different SM1-derived peptides. Error bars represent the standard deviation of technical quadruplicates. The variants F871A and L943A were not stable and therefore could not be investigated (for melting points of the alanine variants, see Table S2).



changes could not be adequately addressed. However, cyclic peptides, which were modelled on the basis of the horseshoe-shaped linear SP1-peptide in the crystal structure, showed very similar binding modes (Figure 1). A closer look reveals almost perfect overlap for peptides SP1 (in PDB-ID 5ZOO), cA-SM1-E, cF-SM1-E, and cV-SM1-E, while peptides cW-SM1-E and c-Nal-SM1-E with bulkier residues W and Nal show clearly different binding poses, particularly in the region of the pivotal GSI-motifs (Figure 1B,C). A more detailed analysis of the molecular interactions between the peptides and cHDAC4 revealed eight residues in cHDAC4 (D757, S758, D759, P809, F812, P872, F871, L943) of particular importance. To investigate their role in the molecular recognition of the peptides, these amino acids were selected for an alanine mutation study. Most of these positions (D757, D759, F812, P872, F871) also play a role in HDAC4 binding to SMRT.<sup>15</sup> Docking also indicated that the peptides with large side-chains might be able to form intramolecular interactions.

As shown in Figure 2, most of the alanine-exchange variants were no longer stabilized by the peptides, indicating that the respective residues are essential for peptide binding. The lack of stabilization for most of the variants underlines that the rim of the active site of cHDAC4 is the binding site for the peptides. For cyclic peptides of the cX-SM1-E series, D757 is less important than for the linear precursor peptide and for the smaller cSM1-D, indicating a similar but not identical binding site.

Because the cBpa-SM1-E peptide contained a benzophenone group, we tried to photocrosslink the peptide with cHDAC4 WT to identify protein residues that hydrophobic residues may interact with. In the MALDI-TOF MS analysis of the tryptic digest of the irradiated protein complex, potential photocrosslinked products could not be unambiguously assigned because the peaks were either also present in the MALDI-TOF MS spectra of the untreated protein or, more likely, the result from nonspecific binding, as the fragment in question is spatially separated from the peptide binding site (see Supporting Information section S5 for details). This supports the results of the MD simulation that the hydrophobic side chain is not involved in binding to the protein and instead extends into the solvent.

Further conformational analysis of cHDAC4 WT/GOF-peptide complexes by ion mobility-mass spectrometry (IM-MS) showed that

the collision cross section changed by less than 5% upon peptide binding indicating no large changes to the overall protein fold. (Table S3, Figures S2–S4).

Hydrogen deuterium exchange mass spectrometry (HDX-MS) experiments with the cHDAC4 WT/GOF-peptide complexes indicated that, depending on the cyclic peptide, the protein undergoes small conformational changes that would potentially be undetectable by IM-MS (data not shown). Due to the discontinuous nature of the binding site of the cyclic peptides, changes in deuteration of the individual HDAC4 peptides upon peptide binding are expected to be small and are difficult to detect in the initial HDX-MS data set so that further investigation is required.

## 4 | CONCLUSION

Based on the SMRT-motif-1 derived from the binding site of corepressor SMRT to HDAC4, we have systematically developed a series of cyclic peptides that inhibit cHDAC4 activity up to 56 times better than the linear SM1 sequence. Similar to SMRT, these peptides bind to the rim of cHDAC4's active site but do not engage D757, one of SMRT's hot spots. Binding to the rim rather than the interior of the active site bears the potential to block access to the active site and specifically disrupt the SMRT/HDAC3/HDAC4-complex without interfering with the function of other HDACs. To test this disruption in vitro, a well-characterized system is required, which will be the focus of future research. Due to cyclization, our peptides seem to be well suited to bind essential amino acids of the discontinuous binding site of HDAC4 and thus stabilize the less stable wildtype form to a considerable extent. With a  $\Delta T_m$  of 5.7°C to 7.9°C, these peptides stabilize cHDAC4 WT substantially better than the GOF variant, which is probably due to the latter's greater intrinsic stability. The collision cross-section of the protein-peptide complexes showed only minor differences to that of the apo protein. Small conformational effects seen in initial HDX experiments that differ with the side chain of the amino acid added to the N-terminus of the SMRT-motif-1 will be further explored in future work.

## ACKNOWLEDGEMENTS

We thank Janna Treber for the synthesis of the TAMRA-SM1 peptide and for performing the fluorescence polarization assay with it and cHDAC4 WT during her bachelor thesis. The authors acknowledge support by the mass spectrometry core facility team of the Chemistry Department at TU Darmstadt for measurements of the MALDI-TOF MS spectra and for funding for the instrument by the German Research Foundation (DFG) through grant no INST 163/445-1 FUGG. Funding for this work was provided by the Hessian Ministry of Higher Education, Research and Arts (HMWK) under the LOEWE project "TRABITA." The Synapt XS instrument was cofunded by the German Research Foundation (DFG; grant number 461372424). Open Access funding enabled and organized by Projekt DEAL.

## ORCID

Franz-Josef Meyer-Almes  <https://orcid.org/0000-0002-1001-3249>

Katja Schmitz  <https://orcid.org/0000-0001-9023-318X>

## REFERENCES

- Christensen DG, Xie X, Basisty N, et al. Post-translational protein acetylation: an elegant mechanism for bacteria to dynamically regulate metabolic functions. *Front Microbiol.* 2019;10:1604. doi:10.3389/fmicb.2019.01604
- Li G, Tian Y, Zhu W-G. The roles of histone deacetylases and their inhibitors in cancer therapy. *Front Cell Dev Biol.* 2020;8:576946. doi:10.3389/fcell.2020.576946
- Park S-Y, Kim J-S. A short guide to histone deacetylases including recent progress on class II enzymes. *Exp Mol Med.* 2020;52(2):204-212. doi:10.1038/s12276-020-0382-4
- Gallinari P, Di Marco S, Jones P, Pallaoro M, Steinkühler C. HDACs, histone deacetylation and gene transcription: from molecular biology to cancer therapeutics. *Cell Res.* 2007;17(3):195-211. doi:10.1038/sj.cr.7310149
- Bannister AJ, Kouzarides T. Regulation of chromatin by histone modifications. *Cell Res.* 2011;21(3):381-395. doi:10.1038/cr.2011.22
- Fischle W, Dequiedt F, Hendzel MJ, et al. Enzymatic activity associated with class II HDACs is dependent on a multiprotein complex containing HDAC3 and SMRT/N-CoR. *Mol Cell.* 2002;9(1):45-57. doi:10.1016/s1097-2765(01)00429-4
- Seto E, Yoshida M. Erasers of histone acetylation: the histone deacetylase enzymes. *Cold Spring Harb Perspect Biol.* 2014;6(4):a018713. doi:10.1101/cshperspect.a018713
- Wang Z, Qin G, Zhao TC. HDAC4: mechanism of regulation and biological functions. *Epigenomics.* 2014;6(1):139-150. doi:10.2217/epi.13.73
- Cuttini E, Goi C, Pellarin E, Vida R, Brancolini C. HDAC4 in cancer: a multitasking platform to drive not only epigenetic modifications. *Front Mol Biosci.* 2023;10:1116660. doi:10.3389/fmolb.2023.1116660
- Bottomley MJ, Lo Surdo P, Di Giovine P, et al. Structural and functional analysis of the human HDAC4 catalytic domain reveals a regulatory structural zinc-binding domain. *J Biol Chem.* 2008;283(39):26694-26704. doi:10.1074/jbc.M803514200
- Lahm A, Paolini C, Pallaoro M, et al. Unraveling the hidden catalytic activity of vertebrate class IIa histone deacetylases. *Proc Natl Acad Sci U S A.* 2007;104(44):17335-17340. doi:10.1073/pnas.0706487104
- Brancolini C, Gagliano T, Minisini M. HDACs and the epigenetic plasticity of cancer cells: target the complexity. *Pharmacol Ther.* 2022;238:108190. doi:10.1016/j.pharmthera.2022.108190
- Martin M, Kettmann R, Dequiedt F. Class IIa histone deacetylases: regulating the regulators. *Oncogene.* 2007;26(37):5450-5467. doi:10.1038/sj.onc.1210613
- Jayathilaka N, Han A, Gaffney KJ, et al. Inhibition of the function of class IIa HDACs by blocking their interaction with MEF2. *Nucleic Acids Res.* 2012;40(12):5378-5388. doi:10.1093/nar/gks189
- Kim GS, Jung H-E, Kim J-S, Lee YC. Mutagenesis study reveals the rim of catalytic entry site of HDAC4 and -5 as the major binding surface of SMRT corepressor. *PLoS ONE.* 2015;10(7):e0132680. doi:10.1371/journal.pone.0132680
- Aranda A, Pascual A. Nuclear hormone receptors and gene expression. *Physiol Rev.* 2001;81(3):1269-1304. doi:10.1152/physrev.2001.81.3.1269
- Hudson GM, Watson PJ, Fairall L, Jamieson AG, Schwabe JWR. Insights into the recruitment of class IIa histone deacetylases (HDACs) to the SMRT/NCoR transcriptional repression complex. *J Biol Chem.* 2015;290(29):18237-18244. doi:10.1074/jbc.M115.661058
- Park S-Y, Kim GS, Hwang H-J, et al. Structural basis of the specific interaction of SMRT corepressor with histone deacetylase 4. *Nucleic Acids Res.* 2018;46(22):11776-11788. doi:10.1093/nar/gky926
- Gray SG. Targeting Huntington's disease through histone deacetylases. *Clin Epigenetics.* 2011;2(2):257-277. doi:10.1007/s13148-011-0025-7
- Bürli RW, Luckhurst CA, Aziz O, et al. Design, synthesis, and biological evaluation of potent and selective class IIa histone deacetylase (HDAC) inhibitors as a potential therapy for Huntington's disease. *J Med Chem.* 2013;56(24):9934-9954. doi:10.1021/jm4011884
- Wu Y, Hou F, Wang X, Kong Q, Han X, Bai B. Aberrant expression of histone deacetylases 4 in cognitive disorders: molecular mechanisms and a potential target. *Front Mol Neurosci.* 2016;9:114. doi:10.3389/fnmol.2016.00114
- Ho TCS, Chan AHY, Ganesan A. Thirty years of HDAC inhibitors: 2020 insight and hindsight. *J Med Chem.* 2020;63(21):12460-12484. doi:10.1021/acs.jmedchem.0c00830
- Bondarev AD, Attwood MM, Jonsson J, Chubarev VN, Tarasov VV, Schiöth HB. Recent developments of HDAC inhibitors: emerging indications and novel molecules. *Br J Clin Pharmacol.* 2021;87(12):4577-4597. doi:10.1111/bcp.14889
- Di Giorgio E, Gagliostro E, Brancolini C. Selective class IIa HDAC inhibitors: myth or reality. *Cell Mol Life Sci.* 2015;72(1):73-86. doi:10.1007/s00018-014-1727-8
- Yang F, Zhao N, Ge D, Chen Y. Next-generation of selective histone deacetylase inhibitors. *RSC Adv.* 2019;9(34):19571-19583. doi:10.1039/c9ra02985k
- Shen S, Kozikowski AP. Why hydroxamates may not be the best histone deacetylase inhibitors—what some may have forgotten or would rather forget? *ChemMedChem.* 2016;11(1):15-21. doi:10.1002/cmdc.201500486
- Tilekar K, Hess JD, Upadhyay N, et al. Thiazolidinedione "magic bullets" simultaneously targeting PPAR $\gamma$  and HDACs: design, synthesis, and investigations of their in vitro and in vivo antitumor effects. *J Med Chem.* 2021;64(10):6949-6971. doi:10.1021/acs.jmedchem.1c00491
- Schweipert M, Jänsch N, Upadhyay N, et al. Mechanistic insights into binding of ligands with thiazolidinedione warhead to human histone deacetylase 4. *Pharmaceuticals.* 2021;14(10):1032. doi:10.3390/ph14101032
- Lobera M, Madauss KP, Pohlhaus DT, et al. Selective class IIa histone deacetylase inhibition via a nonchelating zinc-binding group. *Nat Chem Biol.* 2013;9(5):319-325. doi:10.1038/nchembio.1223
- Higuchi R, Krummel B, Saiki RK. A general method of in vitro preparation and specific mutagenesis of DNA fragments: study of protein and DNA interactions. *Nucleic Acids Res.* 1988;16(15):7351-7367. doi:10.1093/nar/16.15.7351



31. Vølund A. Application of the four-parameter logistic model to bioassay: comparison with slope ratio and parallel line models. *Biometrics*. 1978;34(3):357-365. doi:[10.2307/2530598](https://doi.org/10.2307/2530598)
32. Cheng Y, Prusoff WH. Relationship between the inhibition constant (K1) and the concentration of inhibitor which causes 50 per cent inhibition (I50) of an enzymatic reaction. *Biochem Pharmacol*. 1973; 22(23):3099-3108. doi:[10.1016/0006-2952\(73\)90196-2](https://doi.org/10.1016/0006-2952(73)90196-2)
33. Micsonai A, Wien F, Bulyáki É, et al. BeStSel: a web server for accurate protein secondary structure prediction and fold recognition from the circular dichroism spectra. *Nucleic Acids Res*. 2018;46(W1):W315-W322. doi:[10.1093/nar/gky497](https://doi.org/10.1093/nar/gky497)
34. Cardote TAF, Ciulli A. Cyclic and macrocyclic peptides as chemical tools to recognise protein surfaces and probe protein-protein interactions. *ChemMedChem*. 2016;11(8):787-794. doi:[10.1002/cmdc.201500450](https://doi.org/10.1002/cmdc.201500450)
35. White CJ, Yudin AK. Contemporary strategies for peptide macrocyclization. *Nat Chem*. 2011;3(7):509-524. doi:[10.1038/nchem.1062](https://doi.org/10.1038/nchem.1062)
36. Schweipert M, Jänsch N, Sugiarto WO, Meyer-Almes F-J. Kinetically selective and potent inhibitors of HDAC8. *Biol Chem*. 2019;400(6): 733-743. doi:[10.1515/hsz-2018-0363](https://doi.org/10.1515/hsz-2018-0363)
37. Meyners C, Mertens M, Wessig P, Meyer-Almes F-J. A fluorescence-lifetime-based binding assay for class IIa histone deacetylases. *Chemistry*. 2017;23(13):3107-3116. doi:[10.1002/chem.201605140](https://doi.org/10.1002/chem.201605140)

#### SUPPORTING INFORMATION

Additional supporting information can be found online in the Supporting Information section at the end of this article.

**How to cite this article:** Lill A, Schweipert M, Nehls T, et al. Design and synthesis of peptides as stabilizers of histone deacetylase 4. *J Pept Sci*. 2024;30(9):e3603. doi:[10.1002/psc.3603](https://doi.org/10.1002/psc.3603)